MM Science Journal | www.mmscience.eu
ISSN 1803-1269 (Print) | ISSN 1805-0476 (On-line)
Special Issue | CUTTING TOOLS 2024
1st International Conference on Cutting Tools
November 20-22, 2024, Trnava, Slovakia
DOI: 10.17973/MMSJ.2025_06_2025031

CUTTINGTOOLS2024-00011

MICROHARDNESS AND ELASTIC MODULUS OF THIN COATINGS APPLIED VIA PVD AND CVD TECHNIQUES

O. Bilek, J. Knedlova*, A. Audyova
Tomas Bata University in Zlin, Department of Production Engineering, Vavreckova 5669, 76001 Zlin, Czech Republic
*Corresponding author; e-mail: knedlova@utb.cz

Abstract
This study investigates the microhardness and mechanical properties of thin coatings applied to cemented carbide cutting tools. Two primary coating techniques were examined: Physical Vapor Deposition (PVD) and Moderate Temperature Chemical Vapor Deposition (MT- CVD). PVD coatings of titanium carbonitride (TiCN) and aluminium titanium nitride (AlTiN) were applied, along with multi-layer CVD coatings consisting of TiCN, titanium carbide (TiC), and aluminium oxide (Al_2O_3). Depth-sensing indentation (DSI) tests using a Vickers indenter were conducted to determine the microhardness and elastic modulus of the coatings. The Oliver and Pharr method, was employed to analyse load-unload curves, enabling precise evaluation without direct measurement of imprint areas.
The results demonstrated that TiCN coatings applied via PVD exhibited the highest microhardness as a complex is 2857 HVIT and elastic modulus among all tested samples is 649 GPa. This superior performance indicates enhanced wear resistance and mechanical stability, which are critical for extending the lifespan and efficiency of cutting tools. While multi-layer CVD coatings also offered benefits, their overall performance was inferior to that of TiCN PVD coatings.

Keywords:
Microhardness, Cutting Tools, Coatings, PVD, CVD, DSI, Elastic Modulus

1 INTRODUCTION

The performance and life of cutting tools are critical factors in modern manufacturing processes, where efficiency and precision are paramount. Coatings on cutting tools have emerged as a vital component in enhancing tool performance by improving wear resistance, reducing friction, and increasing thermal stability [Sousa 2021a] [Parsi 2020]. In particular, cemented carbide tools have gained widespread use due to their exceptional hardness and toughness, which make them suitable for high-speed machining applications [Iqbal 2006] [Kaladhar 2011].

Coatings such as titanium carbonitride (TiCN) and titanium aluminium nitride (AlTiN) are commonly applied to cemented carbide tools using Physical Vapor Deposition (PVD) techniques [Sousa 2021b] [Sousa3 2021c]. These coatings exhibit high microhardness and excellent mechanical properties, contributing to enhanced tool life and machining performance [Chen 2023] [Mohammed 2021]. For instance, TiCN coatings have been reported to achieve microhardness values ranging from 3000 to 3200 HV, providing significant improvements in wear resistance and tool longevity [Siow 2019] [Colombo-Pulgarín 2021]. Similarly, AlTiN coatings exhibit even higher hardness levels, often exceeding HV 3300, which enhances their ability to withstand high temperatures and mechanical stresses during machining [Mohammed 2021] [Dumkum 2018].

Multilayer coatings, such as TiCN + TiC + Al_2O_3, deposited via Moderate Temperature Chemical Vapor Deposition (MT-CVD), have also shown promise in further improving the wear resistance and thermal stability of cutting tools [Boing 2018] [Boing 2020]. The combination of different layers allows for the exploitation of individual material properties, resulting in coatings with superior performance. The TiC layer contributes to increased hardness and wear resistance, while the Al_2O_3 layer provides excellent thermal stability and oxidation resistance [Zhang 2009] [Panagopoulos 2010]. These multilayer coatings can achieve microhardness values exceeding HV 3500, making them suitable for demanding machining applications [Pogrebnjak 2015] [Wang 2013].

The application of multilayer coatings allows for the combination of different material properties to optimize tool performance under various machining conditions. The alternating layers can provide synergistic effects, enhancing hardness, toughness, and resistance to oxidation and thermal degradation [Pogrebnjak 2015] [Zhang2009]. Understanding the mechanical properties of these coatings, particularly microhardness and elastic modulus, is essential for predicting tool behavior and optimizing coating processes.

The measurement of microhardness and elastic modulus in thin coatings poses significant challenges due to the influence of the substrate material. The Depth Sensing Indentation (DSI) technique, coupled with the Oliver–Pharr method, offers a reliable means to characterize these properties at the nanoscale without direct measurement of the indentation area [Oliver 1992] [Grigoriev 2018]. The use of a Vickers indenter in DSI allows for precise control and analysis of the load–displacement data, enabling the extraction of mechanical properties specific to the coating material [Drobný 2021] [Kiran 2010] [Monka 2022].

Despite the advancements in coating technologies and characterization methods, there remains a need for comprehensive studies that evaluate the mechanical properties of advanced coatings on cemented carbide tools. Such studies are crucial for developing coatings that can meet the increasing demands of high-performance machining applications.

This research presents the experimental results of microhardness and elastic modulus tests of TiCN and AlTiN coatings prepared by PVD, and a multilayer TiCN + TiC + Al_2O_3 coating produced by MT-CVD on cemented carbide cutting tools. The tests were conducted using the instrumented DSI method with a Vickers four-sided indenter. The measured properties were analysed using the Oliver–Pharr method from the load–unload curves without direct measurement of the projected indentation area. This study aims to provide insights into the mechanical behaviour of these coatings, including an overview of the achieved hardness values, contributing to the optimization of coating processes and the development of cutting tools with enhanced performance.

2 MATERIAL AND METHODS

In this study, three types of coated cemented carbide cutting tools were utilized as test samples. All tools were manufactured via powder metallurgy, resulting in an ultra-fine grain structure, and were coated with thin hard layers. Each selected sample possesses specific properties, layer compositions, and distinct applications in machining processes.

2.1 Materials

Sample 1

The first material examined was a replaceable cutting insert (RCI) from Korloy, sign sample 1 (Figure 1), designated as NC3120. The insert is made of cemented carbide with a micro grain structure containing 6 - 12% Co as binder, coated with a multilayer TiCN + TiC + Al_2O_3 coating produced by MT-CVD.

Fig. 1: Cutting insert Korloy.

The bottom layer of TiCN provides adhesion to the substrate and high wear resistance, the intermediate TiC layer offers the highest hardness among the layers, enhancing the overall durability of the coating and the top layer of Al_2O_3 serves as a thermally stable barrier, protecting the tool at elevated temperatures during machining. The geometry of the insert is WNMG080404-HM, commonly used in turning processes for roughing and semi-finishing of steel materials. The cemented carbide substrate belongs to the ISO P25 application group.

Sample 2

The second sample was an indexable cutting insert from Kyocera, sign sample 2 (Figure 2), with the grade designation PR930. The insert material is cemented carbide with a super-fine micro grain structure coating 8 - 12% of Co. A thin, wear-resistant layer of titanium carbonitride (TiCN) was applied to the substrate surface using TiCN coatings are known for their high hardness and toughness, making them suitable for finishing. The geometrical parameters of the insert are VBGT110304FN- Z. These inserts are intended for finishing turning operations of materials with machinability classes ISO P20 and ISO M20, characterized as steels and stainless steels. According to the manufacturer's catalogue, the hardness of this insert is 30 GPa, and the coating hardness, is specified as 16.7 GPa or HV 1700.

Fig. 2: Cutting insert Kyocera.

Sample 3

The third sample examined was mill cutter V7 PLUS (Figure 3) from YG-1 (South Korea). The substrate material of the end mill is ultrafine microstructure cemented carbide with approx. 10% of Co. The substrate surface is coated with a hard PVD AlTiN layer. AlTiN, coatings offer high hardness and thermal stability, suitable for high-speed machining applications. The end mill is designed for milling low to medium hardness materials, with hardness not exceeding HRC 40. Suitable workpiece materials include soft and stainless steels or cast irons, designated by international standards as ISO P, ISO M, and ISO K. The manufacturer does not provide specific hardness values for this coating or its substrate.

Fig. 3: Mill cutter V7 Plus.

2.2 Sample preparation

Prior to the instrumented indentation tests, the samples underwent surface preparation, including cutting, mounting, and polishing. The samples were cut to the required dimensions, and the top layer of the coated tool was removed to expose the cross-section of the coatings. Oblique cuts were employed to better observe the transitions between the coating layers and the substrate (Figure 4).

Fig. 4: Coated samples after metallographic preparation.

The cutting was performed using an Isomet 4000 precision saw by Buehler equipped with a diamond cutting wheel. Optimal cooling during the process was maintained to eliminate thermal effects that could alter the material. The cutting parameters were as follows:

- diamond wheel speed: 1800 rpm
- wheel feed rate: 16 mm · min $^{-1}$.

Mounting was performed to encapsulate the samples within a handling medium, facilitating manipulation of the very small samples and allowing secure clamping in the grinder/polisher during subsequent steps. Hot mounting was chosen due to the high melting temperature of the carbide components, using a SimpliMet 1000 device by Buehler. The samples were placed into the mounting cylinder, which was then filled with phenol-formaldehyde (PF) resin granulate. Under applied temperature and pressure, the resin melted and encapsulated the samples. After cooling, the samples were ready for grinding and polishing. The mounting parameters were:

- material Phenol Formaldehyde (PF) resin
- polymerization temperature 150 °C
- pressure 290 bar
- cycle time 1.5 minutes

Polishing is as crucial as the measurement itself since poor surface quality can negatively affect test results. The aim was to remove the damaged material layer resulting from cutting. Fine grinding and polishing were performed with light pressure to prevent tearing out carbide particles or work hardening due to generated heat. All samples were mounted in a multiple-sample holder and leveled to the same height using a leveling device, ensuring even pressure on the grinding wheel surface for all samples simultaneously. Thermal deformations were suppressed by supplying coolant. The initial steps involved fine grinding using a grinding disc assisted by diamond lapping paste, first with a grain size of 9 µm and then 3 µm. This was followed by final polishing using a polishing cloth, during which no material removal from the sample surface occurred. Each polishing process was carried out under a load of 25 N, with rotational speeds of 30 rpm for fine grinding and 300 rpm for final polishing. The result was a highly smooth surface without defects. Grinding and polishing were performed on an AutoMet 250 grinder/polisher by Buehler. The final preparation parameters were:

- fine grinding
  - grinding disc speed 30 rpm
  - lapping paste grain sizes 9 µm, 3 µm
  - applied force 25 N
- polishing
  - polishing cloth speed 300 rpm
  - applied force 25 N

Due to Korloy's, and Kyocera's, proprietary know-how in manufacturing and coating technologies, specific details regarding application parameters, equipment used, application techniques, coating thickness and number of layers are not disclosed and remain confidential as part of the company's intellectual property.

3 MEASUREMENT

The microhardness and indentation modulus of elasticity of the cutting tools were evaluated for each sample separately. All nanoindentation tests were performed using the Depth Sensing Indentation (DSI) method on a Micro-Combi Tester by CSM Instruments (now part of Anton Paar), in accordance with ISO 14577. A Vickers four-sided diamond indenter with apex angles of 136° was used for the microhardness measurements (Figure 5).

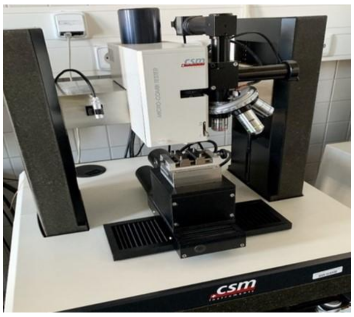

Fig. 5: Micro-Combi tester (CSM Instruments).

Measurements were conducted from the outer edge to the center of the sample, with thirty repetitions for each sample to ensure statistical reliability. During the measurements, the device was connected to a computer that recorded, stored, and evaluated the obtained data. The entire measurement history was graphically processed into indentation curves, representing the load—displacement data.

Microhardness was evaluated using the Oliver–Pharr method, which calculates hardness from the maximum load Fmax and the projected contact area *Ap* without the need for direct measurement of the indentation area [Oliver 1992]. The method provides accurate determination of mechanical properties for thin coatings, accounting for elastic recovery during unloading.

The range of measured values was determined using statistical methods corresponding to a 95% confidence interval, assuming only random errors. The arithmetic mean, standard deviation, and uncertainty range of the measurement values were interpreted according to ISO 3534-1.

The parameters used for the hardness tests were set as follows:

- number of measurements 30 repetitions
- test load 0.5 N
- loading rate 1N · min $^{-1}$
- unloading rate 1N · min $^{-1}$
- dwell time at maximum load 12 s

From the number of thirty measured indentations, the arithmetic mean was calculated, the value of which characterizes the degree of indentation hardness H_{IT}, Vickers microhardness HV_{IT} and indentation modulus of elasticity E_{IT} of each examined sample. The results were obtained by instrumented test for TiCN, AlTiN and TiCN+TiC+Al_2O_3 films deposited on cemented carbide substrates. Measurement results can be negatively affected by errors that reflect the action of many factors. They include influences caused by the measuring instrument or the surface properties of the samples under examination. In the case of a measuring instrument, the influence on the data is caused by temperature fluctuations, the determination of the first dent point, the rigidity of the instrument or the geometry of the indenter. The surface property of the tested samples is significantly affected by the shape of the indentation, which is related to elastic-plastic deformations around the dent. Other factors are the effects of the size of the indentation called ISE (Indentation Size Effect), residual stresses and the quality of the prepared surface of the tested material or the influence of the substrate on the results. Since the testing of the samples was carried out from the outer edge to the centre, it can be expected that the results of the mechanical properties of the thin films will be influenced mainly by the base material, i.e. the substrate. Each resulting value obtained by the average of the measured quantities is also burdened with the variance of random errors.

3.1 Measurement of Indentation Hardness

It is evident that the highest hardness value $H_{IT0.5}$, in the case of the sample 1 (Figure 6), was recorded at the first dent and at the shortest distance h_m from the outer edge. Subsequently, at the next point, the hardness decreases sharply, and then this downward trend gradually continues as the dent distance increases. The maximum measured hardness of 48 GPa is at a distance of 838 nm. The lowest hardness of 14.9 GPa was measured at a distance of 1272 nm. The solid line shows the average value of the indentation hardness, which is 25.3 GPa, which is closest to the point 1013 nm from the edge. The confidence rate determined by the coefficient of determination R^2 is approximately 90.7%.

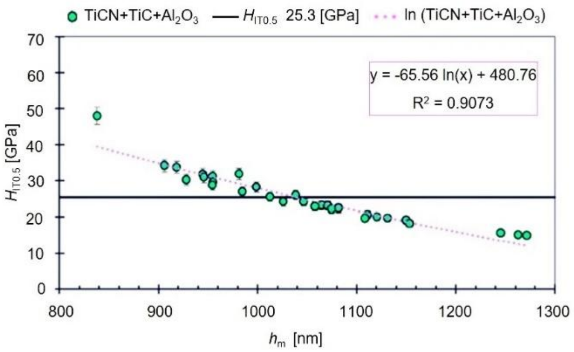

Fig. 6: Dependence of indentation hardness on indentation distance - roughing cutting insert

For the sample 2 (Figure 7), the greatest hardness ($H_{IT0.5}$) of 64.3 GPa was achieved at the first dent point 680 nm from the edge, which was determined as the nearest starting point. The lowest measured hardness value of 15.7 GPa was at a distance (h_m) of 1294 nm. The variance of the measured hardness, as with the sample 1, was achieved around the average value of the indentation hardness, which is 30.3 GPa, as indicated by a solid linear line. Due to the large variance around the regressive logarithmic curve, the behaviour of the indentation hardness is explained only by 88.4%.

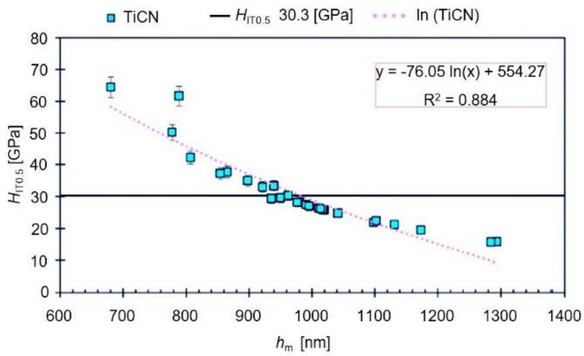

Fig. 7: Dependence of indentation hardness on indentation distance - finishing cutting insert

Unlike the previous dependencies, the end sample 3 (Figure 8) has a lower hardness response around the average value and regressive logarithmic curve. The results thus determine 94.5% reliability. The highest hardness of 42.8 GPa was, as in the previous cases, measured at the shortest specified distance of 824 nm. The last point corresponds to the lowest hardness of $H_{IT0.5}$, namely 23.1 GPa at a maximum distance h_m of 1059 nm and means a decrease in hardness by 46%. The closest to the average calculated value of the v-indentation hardness of 28.2 GPa is at a point 977 nm away.

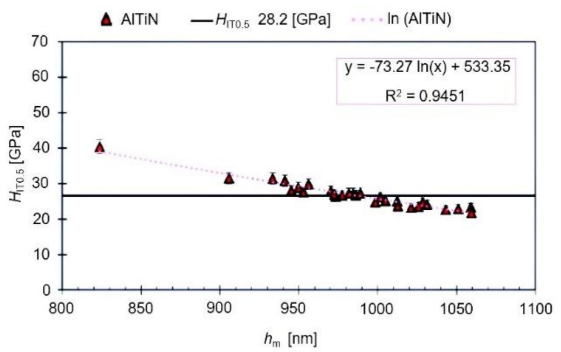

Fig. 8: Dependence of indentation Vickers hardness on indentation distance - mill cutter

The results of the Vickers indenter indentation measurements clearly show the hardness (Figure 9) predominance (H_{IT}) of the TiCN-coated sample 2, with a hardness of 30.3 ± 2.1 GPa. The second hardest tool was the sample 3 AlTiN-coated end mill with a hardness of 28.2 ± 0.7 GPa. The lowest hardness of 25,3 ± 1,3 GPa is achieved in the sample 1 insert with a multilayer coating TiCN+TiC+Al_2O_3. The multilayer coating recorded the greatest hardness decrease of approximately 16.5% from the hardest TiCN layer and the AlTiN coated tool by only 6.9%. Since the manufacturer of the TiCN-coated insert states a hardness of 30 GPa for this layer, it can be stated that the measurement was carried out without the influence of the substrate. Similarly, it also states the hardness of the substrate to be 16.7 GPa, which implies that the application of the protective TiCN layer increased the hardness of the base material by 81.4%. The absence of information cannot constructively compare how the hardness values differ between the other two cutting tool manufacturers.

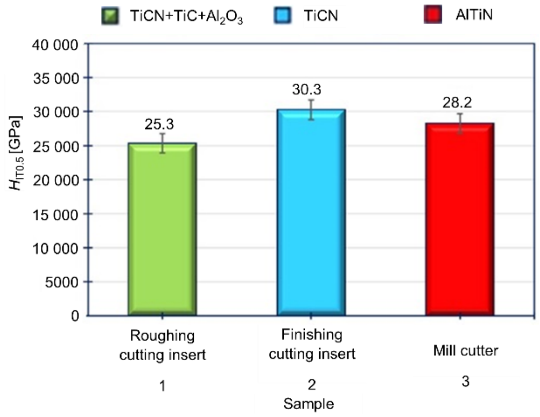

Fig. 9: Indentation hardness H_{IT}

3.2 Measurement of Indentation Microhardness

With the first indentation at a distance (h_m) of 838 nm, the microhardness ($HV_{IT0.5}$) of the folded TiCN+TiC+Al_2O_3 layer reached a value $HV_{IT0.5}$ 4529. The downward tendency to lose hardness is interrupted in several places, and there can be many reasons for such a behavioural situation. The most likely variant is a change in the coating layer in a multilayer system. The smallest microhardness value $HV_{IT0.5}$ 1410 was measured at the last point in the longest interval of the indentation distance of 1272 nm. The average mean value of micro-hardness $HV_{IT0.5}$ 2393 corresponds most closely to a point distant from the edge of 1013 nm, see Figure 10.

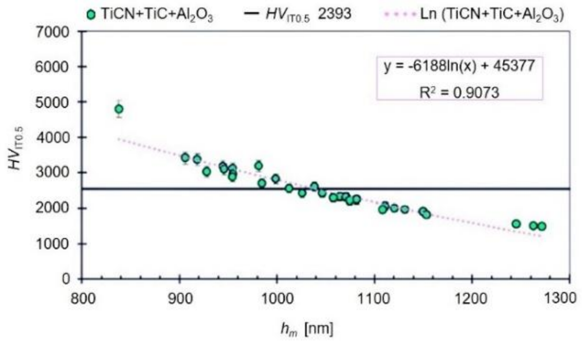

Fig. 10: Dependence of indentation Vickers microhardness on indentation distance - roughing cutting insert.

The greatest hardness $HV_{IT\,0.5}$ 6073 was again found at the first contact point with a distance of 680 nm from the edge (Figure 11). The average mean value $HV_{IT\,0.5}$ 2857 is closest to the point 963 nm away and at the longest indentation distance of 1294 nm a hardness $HV_{IT\,0.5}$ 1479 was measured. The hardness behaviour by the regression curve is explained only 88.4%.

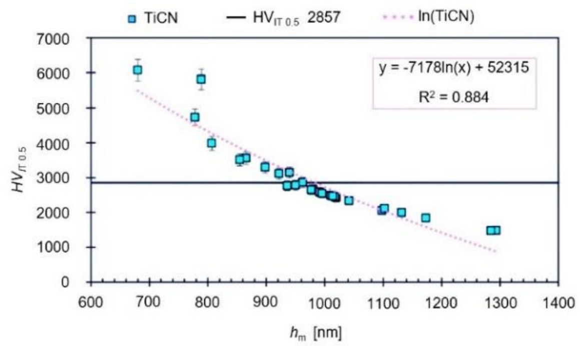

Fig. 11: Dependence of indentation Vickers microhardness on indentation distance - finishing cutting insert

The Vickers hardness point range of the end sample 3 (Figure 12) is closest to its mean $HV_{IT0.5}$ 2665. At the point of first contact of 824 nm, the largest measured value of Vickers hardness is again $HV_{IT0.5}$ 4036. At the next point, a sharp decrease $HV_{IT0.5}$ 897 is observed, and then there is a very gradual decrease in hardness with increasing indentation distance. The smallest Vickers hardness value $HV_{IT0.5}$ 2179 was measured at the last point, which corresponds to the furthest point of the indentation of 1059 nm. The confidence rate determined by the logarithmic regression curve is 94.5%.

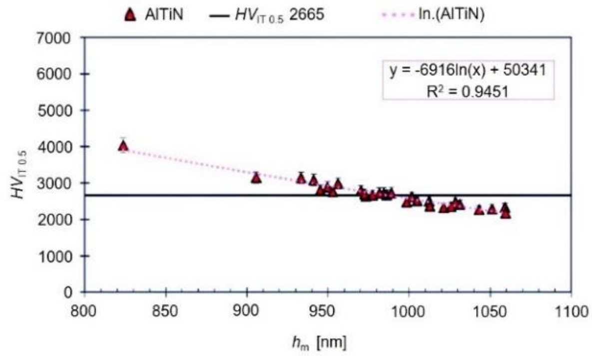

Fig. 12: Dependence of indentation Vickers microhardness on indentation distance - mill cutter

The highest hardness is again observed (Figure 13) in the TiCN layer deposited by PVD on the surface of the Kyocera indexable insert. The hardness of this insert reaches $HV_{IT0.5}$ 2857 ± 199. An end mill with an AlTiN PVD coating from YG-1 and a hardness $HV_{IT\,0.5}$ 2665 ± 68 showed a 6.7% decrease in hardness compared to TiCN. Korloy is indexable insert with MT-CVD multilayer coating TiCN+TiC+Al_2O_3 came in third place with a hardness $HV_{IT\,0.5}$ 2393 ± 121, a decrease of 9.9%. In the case of the TiCN layer, the manufacturer specifies a substrate hardness *HV* 1700, so it can be confirmed that the application of the protective layer effectively increased the hardness of the base material by 59.5%. In the case of a multi-layer coating, the manufacturer's catalogue values for the hardness of the individual elements range from *HV* 3000 for the Al_2O_3 element and *HV* 3200 for the TiC element. However, the method of determining these values is not specified in more detail either in terms of measurement parameters (maximum test load) or material (bulk mixture, coating). In our case, the measured value was 22% lower. The manufacturer of the insert with the AlTiN layer does not provide any information on this layer.

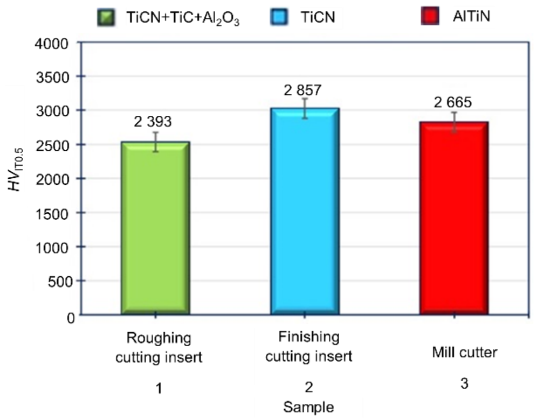

Fig. 13: Indentation microhardness $HV_{IT0.5}$.

The interdependence models presented by graphs are a useful indicator of hardness loss over the course of changing dent sites. Each indentation is marked in a graph point by point with the hardness of the coating, determining the distance at which the given hardness value was measured. If the thickness of the coating layers is known, it would be possible to determine exactly at which point the substrate is already influencing the results. In a multilayer system, the layer thickness information would additionally allow the point distance to be linked to the layer.

3.3 Measurement of Indentation Modulus Elasticity

The first touch (Figure 14) at a distance of 838 nm from the edge is measured by the highest E_{IT} indentation module with a size of 832 GPa. The elastic response of the coating decreases irregularly during the test to the lowest measured value of 617 GPa at a distance of 1153 nm from the edge. The irregularity is most likely due to the microstructure and density of the individual layers. Furthermore, it must be considered that the results have been extracted from the maximum load and penetration depth over the entire interval. And since the depth of penetration is not specified in detail in this work, it is obvious that the result of each dent is directly affected by the depth. During a series of measurements, the indentation module showed a decrease of 355 GPa at an interval of 434 nm. The variance around the regression curve determines the confidence rate of only 60.3%.

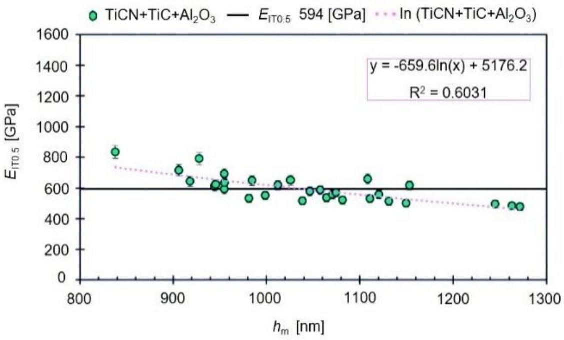

Fig. 14: Dependence of indentation modulus of elasticity on indentation distance - roughing cutting insert.

The indentation modulus elasticity E_{IT} (Figure 15) describes the behaviour of the indentation module as a function of the distance of a TiCN-coated insert. The largest 1400 GPa indentation module was found in the first dent 680 nm away from the edge. The outermost point of 1294 nm showed the lowest modulus of elasticity of 377 GPa. With a difference in the indentation distance of 613 nm, the total module decreased by 1023 GPa. The large dispersion of points around the mean value of $E_{IT0.5}$ with value 649 GPa is described by a regressive logarithmic curve determining the degree of confidence of the predicted data of 88.5%.

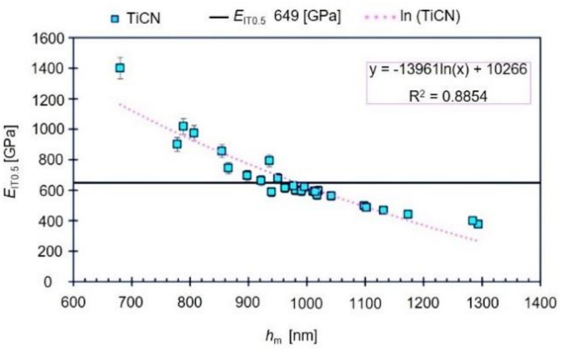

Fig. 15: Dependence of indentation modulus of elasticity on indentation distance - finishing cutting insert.

At the first and last points (Figure 16) distant from 824 and 1059 nm, sizes of 824 and 497 GPa were found, characterizing the highest and lowest values of the indentation module. A typical downward trend towards the centre of the sample is described by a logarithmic curve with a confidence rate of 71.6%. The variance and irregular decline of points around the mean value of the 606 GPa indentation modules is most likely attributable to the effects of the depth of the indentation.

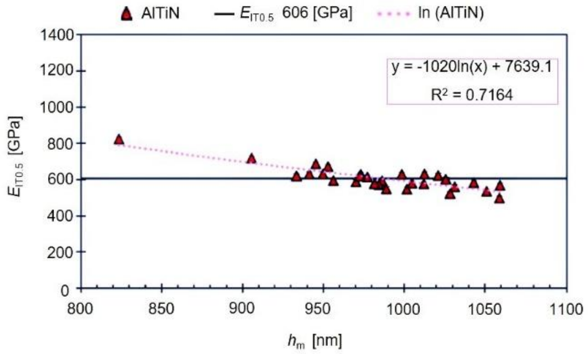

Fig. 16: Dependence of indentation modulus of elasticity on indentation distance - mill cutter.

The E_{IT} values of the indentation modulus follow the elastic response of the material, they are related to its elastic properties.

For TiCN-coated Kyocera finishing inserts, the highest value of the indentation modulus was calculated to be $E_{IT0.5}$ 649 ± 39 [GPa], Figure 17. A 6.6% smaller indentation modulus was found in a coated AlTiN-coated end mill with an $E_{IT0.5}$ 606 ± 11 [GPa]. The smallest indentation modulus was observed in the Korloy multilayer finishing insert with TiCN+TiC+Al2O3, the achieved value $E_{IT0.5}$ 594 ± 16 [GPa] is 8.5% lower than that of the TiCN layer.

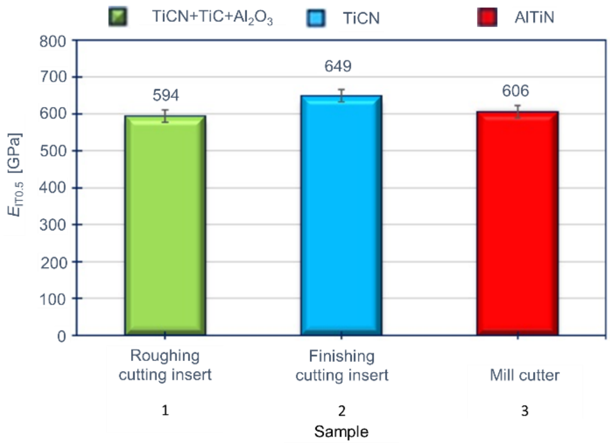

Fig. 17: Indentation modulus elasticity

3.4 Bearer and Plastic Deformation Ratios

The ratio of Hardness, Microhardness and Modulus Elasticity represents an indicator of resistance in tribological operations.

Hardness-modulus ratio ($H_{IT} \cdot E_{IT}^{-1}$) is related to the elastic behaviour of the coating layers in the sense of elastic stress leading to failure.

Resistance to plastic deformation is represented by the parameter $H_{IT}^3 \cdot E_{IT}^{-2}$.

Comparison of the indentation hardness as a function of the indentation module (Figure 18) demonstrates the typical behaviour of the indentation module, which increases with increasing hardness for all examined layers.

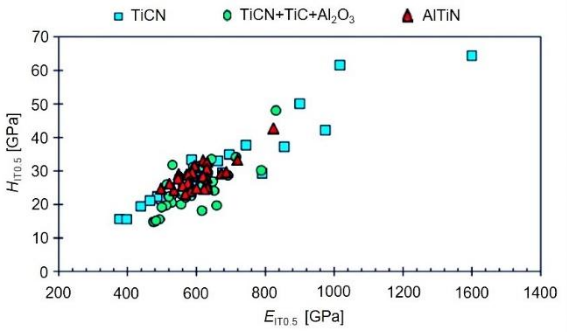

Fig. 18: Dependence of indentation modulus of hardness on indentation modulus of elasticity.

The $H_{IT} \cdot E_{IT}^{-1}$ results should be an indicator of the plastic resistance to the contact of the tool with the surface. Mean $H \cdot E^{-1}$ values of 0.042, 0.046 and 0.047 were determined for the films respectively for TiCN+TiC+Al2O3, TiCN and AlTiN. It is clear from the results that the AlTiN and TiCN layers ended up best, but the values do not differ significantly. However, this does not prove increased resistance to damage to the coating. On the contrary, according to the studies included in [Chen 2019], it was shown that values with an $H_{IT} \cdot E_{IT}^{-1}$ ratio lower than 0.1 showed cracking or cracking in the coating layer, Figure 19.

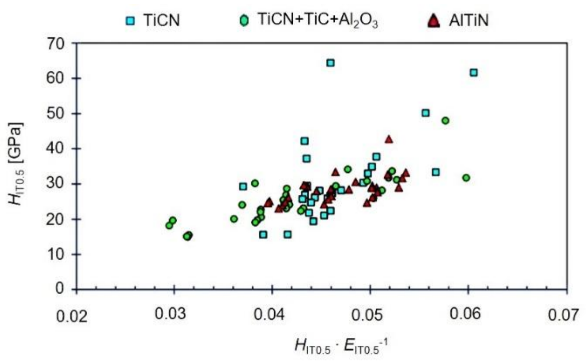

Fig. 19: Dependence of indentation hardness on ratio modulus plasticity.

The dependence of the indentation hardness on the plastic deformation resistance parameter shows the relationship between the hardness and the parameter $H_{IT}^{3} \cdot E_{IT}^{-2}$ related to resistance to plastic deformation. Values $H_{IT}^{3} \cdot E_{IT}^{-2}$ were obtained by average over the whole H_{IT} and E_{IT} intervals and their size is for TiCN+TiC+Al_2O_3 (0.054), TiCN (0.068) and AlTiN (0.063). Greater resistance will be observed in samples with a higher ratio $H_{IT}^{3} \cdot E_{IT}^{-2}$, which in this case is detected at the TiCN layer, Figure 20.

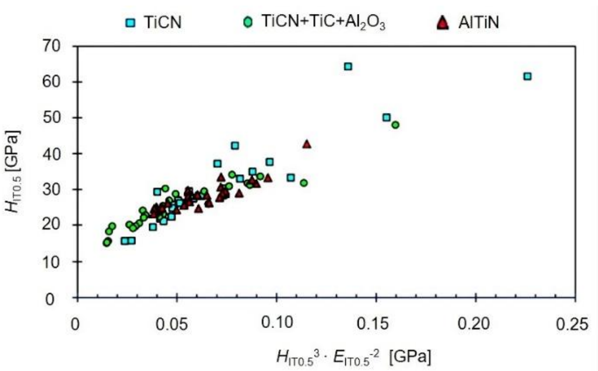

Fig. 20: Dependence of indentation hardness on the resistance to plastic deformation

4 DISCUSION OF RESULTS

The entire surface component containing TiCN layer exhibited the highest Vickers hardness (HV_{IT} 2857). The elastic modulus was highest for the TiCN layer (649 GPa). This ratio, an indicator of the elastic resilience of the layers, was highest for AlTiN (0.047), closely followed by TiCN (0.046). The TiCN layer demonstrated the highest $H^3 \cdot E^{-2}$ ratio (0.068), Figure 21,and also in Table 1.

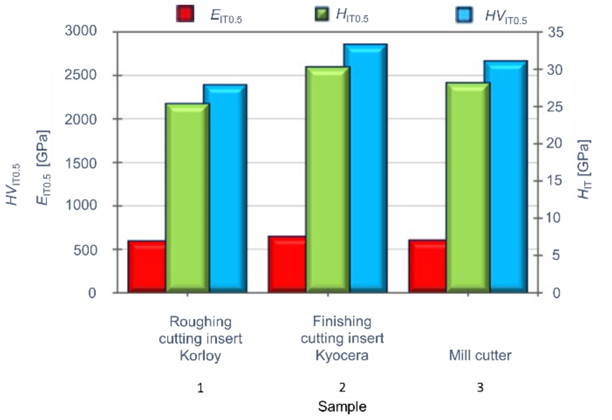

Fig. 21: Comparison of samples with mechanical test results.

TiCN layer demonstrated the best microhardness and modulus of elasticity compared to other coatings. Coatings applied through MT-CVD, particularly multilayer compositions, showed improved overall durability and mechanical performance. DSI testing accurately characterized mechanical properties without direct measurement of the indentation area. TiCN exhibited the highest $H \cdot E^{-1}$ and $H^3 \cdot E^{-2}$ values, suggesting superior performance under mechanical stress. Models allow prediction of mechanical characteristics - surface microhardness - without interference from the substrate or transitional layers.

5 SUMMARY

In this study, thin coatings of TiCN, AlTiN, and a multilayer system (TiCN + TiC + Al_2O_3) deposited on cemented carbide substrates were characterized using depth-sensing indentation to determine their microhardness and elastic modulus. The results of entire surface component indicate that TiCN (PVD) achieved the highest overall hardness (approximately HV_{IT} 2857) and modulus of elasticity (about 649 GPa), suggesting superior wear resistance and mechanical stability. The entire surface component containing AlTiN (PVD) followed closely, exhibiting slightly lower hardness and modulus while still offering robust performance. The multilayer MT-CVD coating (TiCN + TiC + Al_2O_3) displayed the lowest hardness as the entire system among the three tested systems, likely due to the interplay of multiple layers and substrate influences.

Notably, the TiCN coating demonstrated the most favourable balance between hardness and elasticity, reflected in its higher ratios of $H \cdot E^{-1}$ and $H^3 \cdot E^{-2}$ - both recognized indicators of a coating’s ability to withstand plastic deformation under high stress. Although the multilayer CVD system provided a thermally stable top layer (Al_2O_3), its aggregated mechanical response was somewhat diminished compared to the TiCN and AlTiN single-layer coatings. These findings underscore the importance of carefully selecting the coating material and deposition technique to optimize tool life and performance in demanding machining applications.

6 REFERENCES

[Boing 2018] Boing, D., de Oliveira, A. J. and Schroeter, R. B. Limiting Conditions for Application of PVD (TiAlN) and CVD (TiCN/Al2O3/TiN) Coated Cemented Carbide Grades in the Turning of Hardened Steels. Wear, 2018, 416–417, pp. 54–61. ISSN 0043-1648.

[Boing 2020] Boing, D., de Oliveira, A. J. and Schroeter, R. B. Evaluation of Wear Mechanisms of PVD and CVD Coatings Deposited on Cemented Carbide Substrates Applied to Hard Turning. The International Journal of Advanced Manufacturing Technology, 2020, 106(11–12), pp. 5441–5451. ISSN 0268-3768.

[Chen 2023] Chen, S., et al. Boosting Mechanical Properties of W6Mo5Cr4V2 Alloy Fabricated by Directed Energy Deposition Through Tempering Heat Treatment. Steel Research International, 2023, 94(12). ISSN 1611-3683.

[Colombo-Pulgarin 2021] Colombo-Pulgarin, J. C., et al. Mechanical and Chemical Characterisation of TiN and AlTiSiN Coatings on a LPBF Processed IN718 Substrate. Materials, 2021, 14(16), p. 4626. ISSN 1996-1944.

[Drobny 2021] Drobny P., et al. Evaluation of Adhesion Properties of Hard Coatings by Means of Indentation and Acoustic Emission. Coatings, 2021, 11(8), p. 919. ISSN 2079-6412.

[Dumkum 2018] Dumkum, C., Jaritngam, P. and Tangwarodomnukun V. Surface Characteristics and Machining Performance of TiAlN-, TiN- and AlCrN-Coated Tungsten Carbide Drills. Proceedings of the Institution of Mechanical Engineers, Part B: Journal of Engineering Manufacture, 2018, 233(4), pp. 1075-1086.ISSN 0954-4054

[Grigoriev 2018] Grigoriev, S. N., et al. Investigation into Performance of Multilayer Composite Nano-Structured Cr-CrN-(Cr0.35Ti0.40Al0.25) N Coating for Metal Cutting Tools. Coatings, 2021, 11(8), p. 919. ISSN 2079-6412.

[Chen 2019] Chen, X., Du, Y. and Chung, Y. W. Commentary on using *H/E* and H^3/E^2 as proxies for fracture toughness of hard coatings. Thin Solid Films, 2019, Vol. 688, ISSN 0040-6090. DOI:10.1016/j.tsf.2019.04.040.

[Iqbal 2006] Iqbal, A., et al. Influence of Tooling Parameters in High-Speed Milling of Hardened Steels. Key Engineering Materials, 2006, Vols. 315–316, pp. 676–680. ISSN 1013-9826.

[Kaladhar 2011] Kaladhar, M., Subbaiah, K. and Rao, C. S. Performance Evaluation of Coating Materials and Process Parameters Optimization for Surface Quality During Turning of AISI 304 Austenitic Stainless Steel. International Journal of Engineering Science and Technology, 2011, Vol. 3, No. 4. ISSN 0975-5462.

[Kiran 2010] Kiran, M. S. R. N., Kshirsagar, S. D., Krishna, M. G. and Tewari, S. P. Structural, Optical and Nanomechanical Properties of (1 1 1) Oriented Nanocrystalline ZnTe Thin Films. The European Physical Journal Applied Physics, 2010, 51(1), p. 10502. ISSN 1286-0042.

[Mohammed 2021] Mohammed, A. and Hamad, T. I. Assessment of Coating Zirconium Implant Material with Nanoparticles of Faujasite. Journal of Baghdad College of Dentistry, 2021, 33(4), pp. 25–30.

[Monka 2022] Monka, P. P., Monkova, K., Vasina, M., Kubisova, M., Korol, M., & Sekerakova, A. Effect of Machining Conditions on Temperature and Vickers Microhardness of Chips during Planning. Metals, 2022. 12(10). DOI:10.3390/met12101605.

[Oliver 1992] Oliver, W.C., Pharr G. M. An improved technique for determining hardness and elastic modulus using load and displacement sensing indentation experiments. Journal of materials research, *7*(6), 1564-1583.

[Parsi 2020] Parsi, P. K., et al. Machinability Evaluation of Coated Carbide Inserts in Turning of Super-Duplex Stainless Steel. SN Applied Sciences, 2020, 2(11). ISSN 2523-3963.

[Pogrebnjak 2015] Pogrebnjak, A. D., et al. Structure and Properties of Arc Evaporated Nanoscale TiN/MoN Multilayered Systems. International Journal of Refractory Metals and Hard, Materials, 2015, 48, pp. 222–228. ISSN 0263-4368.

[Siow 2019] Siow, P. C., et al. The Study on the Properties of TiC_xN_{1-x} Coatings Processed by Cathodic Arc Physical Vapour Deposition. Tribology – Materials Surfaces & Interfaces, 2019, 13(1), pp. 58–66. ISSN 1751-5831.

[Sousa 2021a] Sousa, V. F. C., et al. Wear Behaviour of Uncoated and Coated Tools in Milling Operations of AMPCO (Cu-Be) Alloy. Applied Sciences, 2021, 11(16), p. 7762. ISSN 2076-3417.

[Sousa 2021b] Sousa, V. F. C., et al. Wear Behaviour and Machining Performance of TiAlSiN-Coated Tools Obtained by Dc MS and HiPIMS: A Comparative Study. Materials, 2021, 14(18), p. 5122. ISSN 1996-1944.

[Sousa 2021c] Sousa, V. F. C., et al. Characteristics and Wear Mechanisms of TiAlN-Based Coatings for Machining Applications: A Comprehensive Review. Metals, 2021, 11(2), p. 260. ISSN 2075-4701.

[Wang 2013] Wang, B. L., Ai, X., Liu, Z. Q. and Liu, J. G. Wear Mechanism of PVD TiAlN Coated Cemented Carbide Tool in Dry Turning Titanium Alloy TC4. Advanced Materials Research, 2013, Vols. 652–654, pp. 2200–2204. ISSN 1022-6680.

[Zhang 2009] Zhang, J., et al. Adhesion and Corrosion Resistance Properties of TiC/Ti (CN)/TiN Multilayer CVD Coatings on 42CrMo Steels. Advanced Materials Research, 2009, Vols. 79–82, pp. 1009–1012. ISSN 1022-6680.

Tab. 1: Comparison of mechanical test results.

sample	$H_{IT0.5}$ [GPa]	$HV_{IT0.5}$	$E_{IT0.5}$ [GPa]	$H_{IT0.5} \cdot E_{IT}^{-1}$	$H_{IT0.5}^{3} \cdot E_{IT0.5}^{-2}$ [GPa]
1 Roughing cutting insert	25.3±1.3	2393±121	594±16	0.042	0.051
2 Finishing cutting insert	30.3±2.1	2857±199	649±39	0.046	0.068
3 Milling cutter	28.2±0.7	2665±68	606±11	0.47	0.063